

Repeat magnetotelluric measurements to monitor The Geysers steam field in northern California

Jared R. Peacock¹, David L. Alumbaugh², Michael A. Mitchell¹, Craig Hartline³

¹U.S. Geological Survey, P.O. Box 158, Moffett Field, CA 94035, USA

²Lawrence Berkeley National Lab, 1 Cyclotron Road Mail Stop 74-316C Berkeley, CA, 94720, USA

³Calpine Corporation, 10350 Socrates Mine Rd, Middletown, CA 95461, USA

jpeacock@usgs.gov

Keywords: Magnetotellurics, Monitoring, The Geysers, Phase Tensor

ABSTRACT

The Geysers in northern California is the world's largest electricity generating steam field. To help understand changes in the steam reservoir, repeat magnetotelluric (MT) measurements are being collected once a year from 2021-2023. These data will be compared and modeled to provide 4D images of changes within the reservoir. Joint inversion with passive seismic data will be done to further constrain changes observed in the geophysical models. This study describes the first repeat survey and provides comparisons with MT data collected in 2017. In April 2021, 41 of the 42 MT stations collected in 2017 were repeated in addition to 14 new stations in the southern part of the steam field. Calculating residual phase tensors from MT responses between the two surveys shows compartmentalized changes within the steam field. Changes are observed at periods longer than one second with the largest changes of up to 30 percent observed at periods of 30 seconds. The residual phase tensors also show good repeatability between the surveys for periods less than one second, with changes on the order of one percent. To model the data, the preferred 3D resistivity volume that resulted from the inversion of the 2017 data is employed as the starting model for inversion of the new data. The two resulting inversion models are then subtracted to identify areas of change within the reservoir.

1. INTRODUCTION

The Geysers in northern California is the world's largest geothermal energy producing steam field (825 MW), where over 60 years of production has significantly modified the steam reservoir. In the mid-1980s, production was 1600 MW but declined due to pressure loss (Stark et al., 2005). To mitigate depletion of the steam field, projects utilizing treated wastewater were developed including the Southeast Geysers Effluent Pipeline (SEGEP) since late 1997 (Brauner & Carlson, 2002), and the Santa Rosa Geysers Recharge Project (SRGRP) since late 2003 (Stark et al., 2005). This has stabilized production whilst adding more complexity to the dynamics of the vapor-dominated field. Further expansion for steam production includes the Enhanced Geothermal System (EGS) Demonstration Project in the northwest portion of The Geysers. The EGS stimulates a deep (>3km), high temperature reservoir (HTR) with measured temperatures up to 400 °C and uses treated wastewater from SRGRP (Garcia, et al., 2016).

In 2017, the first magnetotelluric (MT) survey was collected at The Geysers; the data and resultant 3D electrical resistivity model are detailed in Peacock et al. (2020). One key finding from this study was that quality MT data could be collected in what would appear to be a noisy environment with large powerlines, large injection pipes, and steam pipes. Another key finding was that steam saturation could be estimated from electrical resistivity using a modified Archie's equation (Glover, 2010). Both these findings suggest that repeat MT measurements could assist in characterizing time-dependent variations in the steam field (Peacock et al., 2012).

To help understand these time-dependent subsurface variations, the California Energy Commission has funded a three-year project led by Lawrence Berkeley National Labs to monitor The Geysers geothermal field using constant passive seismic measurements coupled with yearly MT campaigns. The different data sets will be both separately and jointly inverted to provide 3D volumes of resistivity and seismic velocity at three different points in time. This study describes the initial results from the first of three MT surveys collected at The Geysers as part of this project.

2. REPEAT MAGNETOTELLURIC DATA

In April 2021, 41 of the 42 MT sites collected in 2017 were repeated, with an additional 14 sites collected in the southern part of the field (Figure 1). Data were collected with the same data loggers, magnetic sensors, and electrodes where possible. Some locations had to be adjusted due to infrastructure development. Each station included two horizontal orthogonal ANT-4 magnetic induction coils and two orthogonal electrical dipoles with a nominal length of 50 m, dependent on vegetation and topography. Electric potentials were measured with Ag-AgCl Stelth 1 Borin electrodes placed in a saturated canvas bag of bentonite clay to reduce contact resistance, which ranged between ~1-7kOhm. The entire setup was oriented with respect to geomagnetic north using a Brunton compass. All four components were connected to a 5-channel 32-bit ZEN data logger developed by Zonge International. The data were recorded on a repeating schedule of 5 hours and 50 minutes sampling at 256 samples/second, and 10-minutes sampling at 4,096 samples/second. The schedules were set such that all recording instruments recorded the sampling rates synchronously to allow for remote reference processing. Data will be made public upon completion of the project in 2023.

To estimate the MT transfer functions, the robust remote reference bounded-influence processing code was used (BIRRP; Chave and Thomson, 2004). One advantage of this code is that multiple remote references can be used to remove incoherent noise between the stations. This is critically important in a noisy environment like The Geysers. Another advantage of the code is that outliers are downweighted in a robust way through regression and coherency sorting. Each station takes between 15-30 minutes to process depending on input data and program settings.

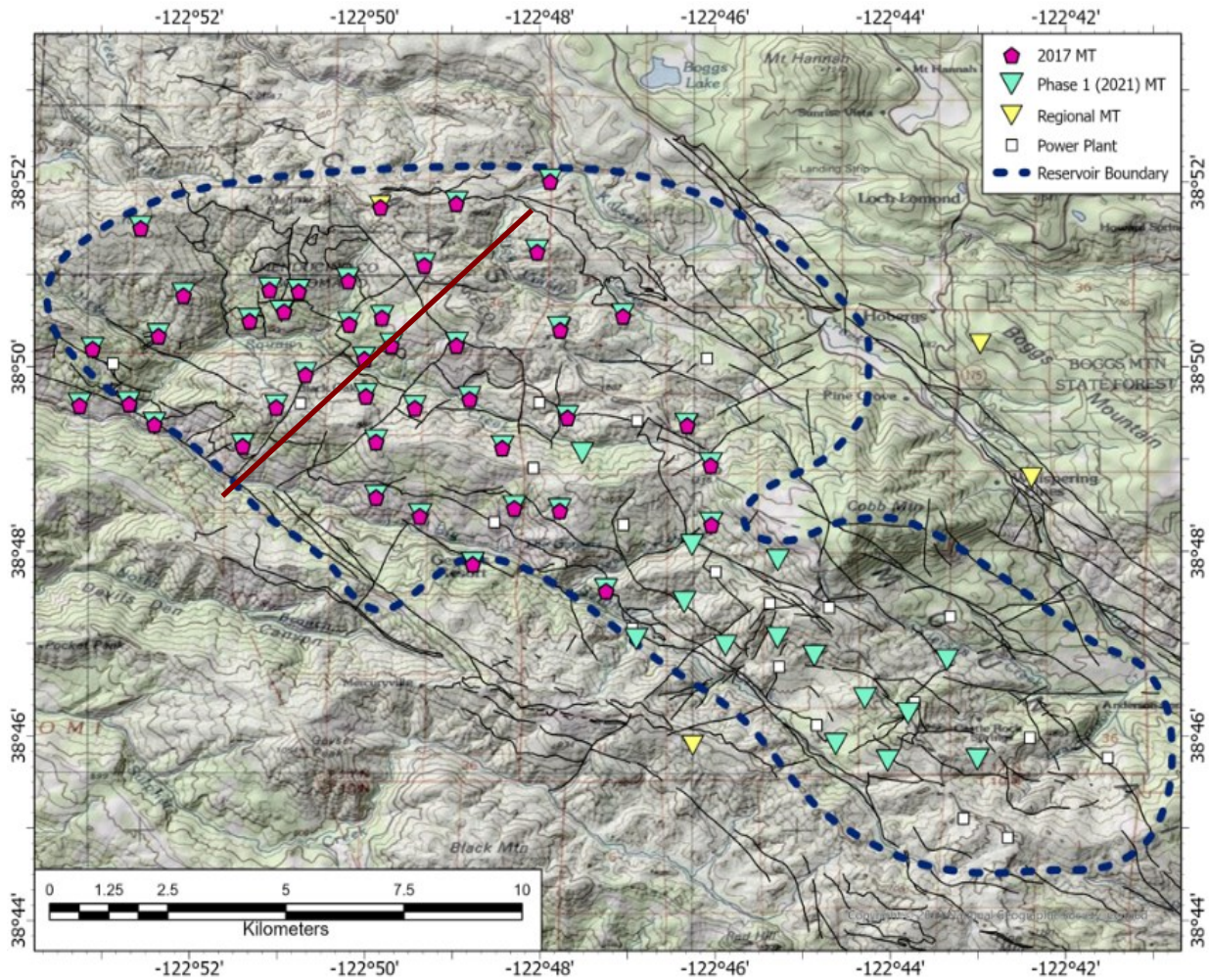


Figure 1: Map of MT stations collected to monitor The Geysers geothermal field. Magenta pentagons: MT stations collected in 2017; cyan triangles: phase 1 MT stations collected in 2021; yellow triangles: regional data collected in 2021. Black lines are mapped faults. Red line: profile line for Figure 4. Map image is the intellectual property of Esri and is used herein under license. Copyright © 2020 Esri and its licensors. All rights reserved.

Comparing the 2021 transfer function estimations to the 2017 data demonstrates that measurements can be accurately repeated (Figure 2). There are a few 2021 stations with new noise sources, and others with better data quality than the 2017 acquisition and processing provided. Near-surface distortions such as changes in soil moisture can cause a static shift in the apparent resistivity. To remove this effect for more accurate comparison between the two campaigns, the first two decades of apparent resistivity for the 2021 data are matched to that of the 2017 data. When comparing transfer functions between 2017 and 2021, the one common feature observed in nearly all processed results is an increase in apparent resistivity and decrease in phase between 1-50 seconds. This would suggest the subsurface increased in resistivity between campaigns. The transfer functions can also be represented as the phase tensor (Caldwell et al., 2004), which are graphically represented as ellipses. The ellipses align and elongate along the preferred direction of electrical current flow. Between 0.01-1 second ellipses are similar between the surveys, then change shape and orientation after five seconds.

A different way of comparing the data sets is to calculate the residual phase tensor (Peacock et al., 2012) as the difference between the two surveys. The residual phase tensor is invariant to near surface distortions and provides directional information on how the subsurface has changed but does not indicate whether the subsurface is becoming more resistive or conductive. Graphically the residual phase tensor

is represented as an ellipse (Figure 3). Each ellipse is viewed in geographic coordinates with the top of the page being North. If the ellipse is circular, this represents equal change in all directions. If the ellipse is elongated, this indicates a larger change in the elongated direction compared to the orthogonal direction. The color represents the percent change between campaigns but does not indicate if the change was more resistive or more conductive. In general, there is a 5-20% change between campaigns at periods longer than 10 seconds. In the northwest Geysers, near the EGS site, variations in subsurface resistivity structure have a southwest-northeast direction, whereas to the east near Caldwell Pines variations have a north-south direction (Figure 3).

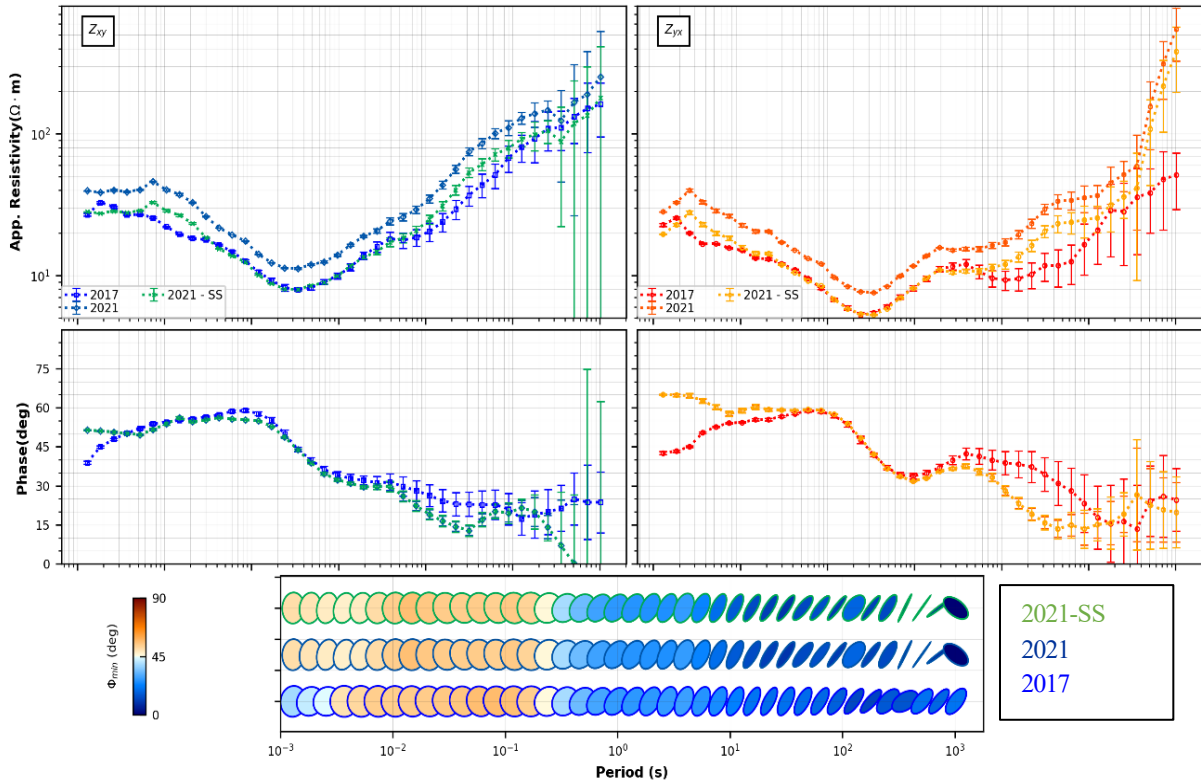


Figure 2: Comparison of an MT response from 2017 (blue and red), 2021 (teal and orange), and 2021 with a static correction (SS) to match 2017 data (green and gold). Top panels are the apparent resistivity, which are affected by near surface distortions, in this case small differences in the soil conditions. This can be corrected by matching the first decades of the 2021 data to the 2017 apparent resistivity. Middle panels show impedance phase, and the bottom panel shows phase tensor representations of the impedance tensor; both impedance phase and phase tensor representations are not affected by near surface distortion. Left panels are components oriented with the electric fields to geographic north and magnetic fields to geographic east. Right panels are components oriented with the electric fields to geographic east and magnetic fields to geographic north. Note the increase in apparent resistivity, dip in phase, and change in phase tensor at around five seconds suggesting the subsurface is becoming more resistive between surveys.

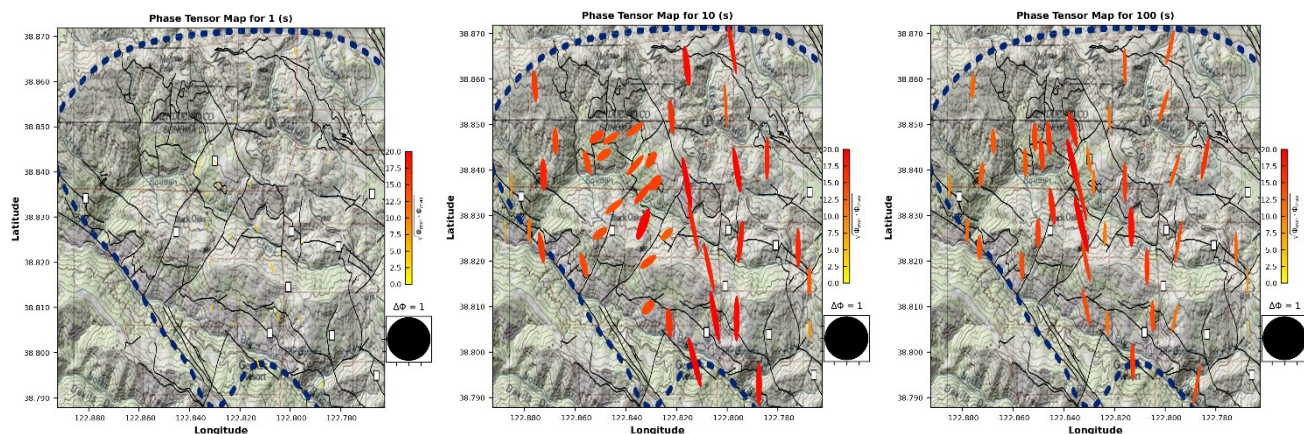


Figure 3: Phase tensor maps for 3 different periods: 1 second (left), 10 seconds (middle) and 100 seconds (right). Minimal change is observed at periods shorter than one second, suggesting that the near surface did not change much between campaigns. However, compartmentalized changes are observed at periods between 1–50 seconds, and a general regional change is observed at periods longer than 50 seconds. Map image is the intellectual property of Esri and is used herein under license. Copyright © 2020 Esri and its licensors. All rights reserved.

3. THREE-DIMENSIONAL INVERSION

In an initial attempt to image variations in subsurface resistivity structure between the two data sets, a 3-D model was developed using ModEM (Egbert & Kelbert, 2012; Kelbert et al., 2014). The initial run employed the final model from 2017 data described in Peacock et al. (2020) as the starting model. This allowed the inversion algorithm to vary the “known” subsurface to fit the 2021 data. An error floor of 5% on the eigenvalues of the impedance tensor was used. A starting lambda value of 100 was used to give the algorithm moderate freedom to change the model where it needed to. A covariance (smoothing parameter) of 0.3 applied in all directions was used as an initial test. Input files were built using MTPy (Kirkby et al., 2019). The inversion ran for 66 iterations on the U.S. Geological Survey high-performance computer Yeti (2019) and reduced the normalized root-mean-square (nRMS) error from 6.3 to 1.6. Comparing the 2017 final model with the 2021 updated model, a coherent increase in resistivity in the steam field is observed (Figure 4). This suggests that steam saturation increased between 2017 and 2021, but this is currently speculative at best. The near surface (top 200 m) became more conductive, likely due to seasonal water content.

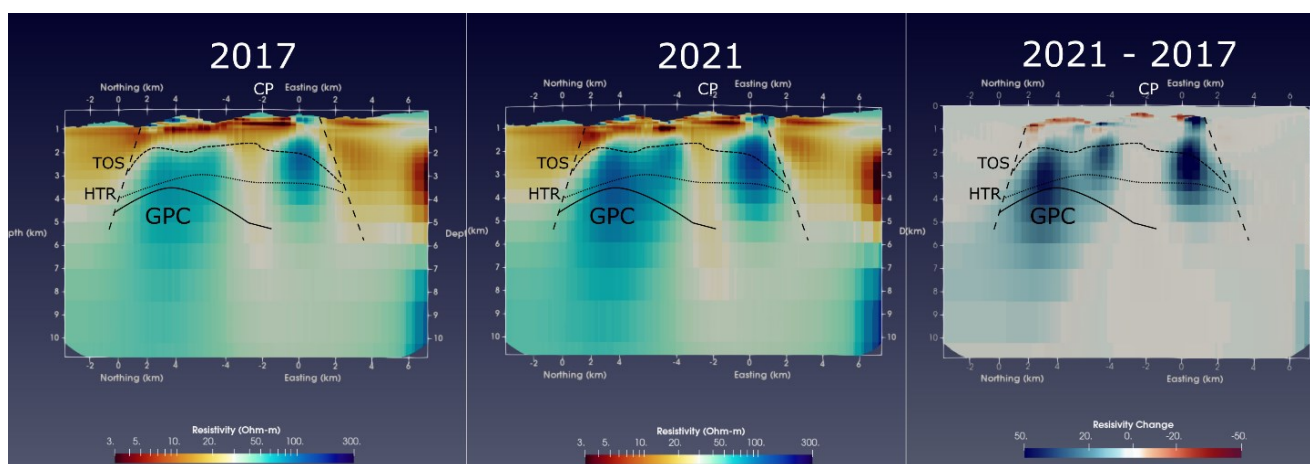


Figure 4: Comparison of 3-D models between the 2017 and 2021 data along a SW-NE profile through Caldwell Pines (Figure 1). Left: final model from Peacock et al. (2020). Middle: 2021 updated model using the 2017 final model as the starting model. Right: Difference between the two models as 2021 minus the 2017 model. TOS: top of steam; HTR: high-temperature reservoir; GPC: Geysers plutonic complex; CP: Caldwell Pines.

5. FUTURE RESEARCH

The 3-D results need to be tested for robustness. This includes changing inversion parameters, using different starting models and prior models, allowing only various parts of the model to change, and a limited forward modeling study where various parts of the model are changed, and synthetic results computed to determine the sensitivity of different parts of the model to the data. The final robust model will then be used as input to a joint inversion with the passive seismic data (see these proceedings Gritto et al. 2022) linked to these MT results using a workflow similar to that described in Um et al. (2014). The next MT field campaign is planned for April of 2022, with the processing workflow described here repeated to image 4-D subsurface variations over The Geysers steam field.

Note: Any use of trade, firm, or product names is for descriptive purposes only and does not imply endorsement by the U.S. Government.

REFERENCES

- Brauner, E., & Carlson, D. C. (2002). *Santa Rosa Geysers Recharge Project: GEO-98-001*. California Energy Commission. Office of Scientific and Technical Information (OSTI). doi:10.2172/897791
- Caldwell, T. G., Bibby, H. M., & Brown, C. (2004). The magnetotelluric phase tensor. *Geophysical Journal International*, 158, 457–469. doi:10.1111/j.1365-246x.2004.02281.x
- Chave, A. D., & Thomson, D. J. (2004). Bounded influence magnetotelluric response function estimation. *Geophysical Journal International*, 157, 988–1006. doi:10.1111/j.1365-246X.2004.02203.x
- Egbert, G. D., & Kelbert, A. (2012). Computational recipes for electromagnetic inverse problems. *Geophysical Journal International*, 189, 251–267. doi:10.1111/j.1365-246X.2011.05347.x
- Garcia, J., Hartline, C., Walters, M., Wright, M., Rutqvist, J., Dobson, P. F., & Jeanne, P. (2016, September). The Northwest Geysers EGS Demonstration Project, California. *Geothermics*, 63, 97–119. doi:10.1016/j.geothermics.2015.08.003
- Glover, P. W. (2010). A generalized Archie's law for n phases. *Geophysics*, 75, E247–E265. doi:10.1190/1.3509781
- Gritto, R., Jarpe, S. P., & Alumbaugh, D. L. (2022). New large-scale passive seismic monitoring at The Geysers geothermal reservoir, CA, USA. *Proceedings, 47th Workshop on Geothermal Reservoir Engineering*, Stanford University, Stanford, CA, 1-11.
- Gritto, R., Yoo, S. H., & Jarpe, S. P. (2013). Three-dimensional seismic tomography at The Geysers Geothermal Field, CA, USA. *38th Workshop on Geothermal Reservoir Engineering, SGP-TR-198*. Stanford.
- Kelbert, A., Meqbel, N. M., Egbert, G. D., & Tandon, K. (2014). ModEM: a modular system for inversion of electromagnetic geophysical data. *Computers & Geoscience*, 66, 40–53. doi:10.1016/j.cageo.2014.01.010
- Kirkby, A., Zhang, F., Peacock, J. R., Hassan, R., & Duan, J. (2019). The MTPy software package for magnetotelluric data analysis and visualisation. *Journal of Open Source Software*, 4, 1358. doi:10.21105/joss.01358
- Peacock, J. R., Earney, T. E., & Schermerhorn, W. (2020a). Magnetotelluric and gravity data from the Northwest Geysers, California. *U.S. Geological Survey data release*. doi:10.5066/P94D21UL
- Peacock, J. R., Earney, T. E., Mangan, M. T., Schermerhorn, W. D., Glen, J. M., Walters, M., & Hartline, C. (2020). Geophysical characterization of the Northwest Geysers geothermal. *Journal of Volcanology and Geothermal Research*, 399, 106882. doi:10.1016/j.jvolgeores.2020.106882
- Peacock, J. R., Thiel, S., Reid, P., & Heinson, G. (2012). Magnetotelluric monitoring of a fluid injection: Example from an enhanced geothermal system. *Geophysical Research Letters*, 39. doi:10.1029/2012gl053080
- Um, E. S., Commer, M., & Newman, G. (2014). A strategy for coupled 3D imaging of large-scale seismic and electromagnetic data sets: application to subsalt imaging. *Geophysics*, 79, ID1-ID13. doi:10.1190/geo2013-0053.1
- USGS Advanced Research Computing. (2019). USGS Yeti Supercomputer. *USGS Yeti Supercomputer*.